Oskar WENGRZYN*

DOI: https://doi.org/JoT2021_09

# Validation of CFD predictions for flow over a full-scale formula student vehicle using PIV in real conditions

**Key words:** *aerodynamics, CFD, validation, PIV, Particle Image Velocimetry, formula student*

Computational Fluid Dynamics (CFD) predictions are becoming an industry standard. They allow for making accurate predictions of complex problems without requiring extensive real-world testing, as well as saving time and money. However, it has been proven many times that the classic Reynolds-averaged Navier – Stokes (RANS) approach has its flaws and fails to provide highly accurate predictions. Even though CFD only approaches a physical solution, which can be reached only in very specific applica-tions, it usually provides enough precision for engineering purposes. To reach a convergence with real-world physics, plenty of factors must be taken into consideration like mesh, boundary conditions, and turbulence models. In order to obtain a CFD simulation that accurately represents real physics, some kind of real-world validation must take place. For aerodynamics, it is usually done in wind tunnels, which are expensive to run but provide controllable conditions to match those specified in CFD. One of the many methods used to validate the calculations is Particle Image Velocimetry (PIV). This study tries to validate CFD of a Formula Student car using PIV, but in real-world conditions, without wind tunnel. The compact size of equipment required for PIV testing and flexibility of CFD boundary conditions allow for that.

## 1. INTRODUCTION

First CFD codes emerged in 1930s, and with many changes along their way, they embedded in engineering world. Along with the growth in computational power available to industrial user, the codes became more advanced and could predict more complex flow behaviors for both heat and fluids. Modern CFD is based on finite volume method where a volume is divided in smaller sections. Nowadays, a mesh of 120 million cells is nothing surprising, while three decades ago, a limited number of institutions would be able to run it. To know how precise our CFD simulation is, a validation is needed. A technique that provides information about the whole flow field velocity is Particle Image Velocimetry (PIV). It uses laser light and seeding particles to calculate the average velocity of a given

* Wroclaw University of Science and Technology

region. Data obtained from these measurements can be used to compare CFD simulation results and adjust the solver parameters or mesh to fit the real case better. PIV allows to measure the real-world case where it is the body that is moving. This gives a unique way to see how the flow field looks while still providing data allowing for its comparison to CFD.


Fig. 1. Formula Student team PWR Racing Team car RTX in front of Van Werven production hall where measurements took place

## 2. BOUNDARY CONDITIONS

Boundary conditions were chosen using best practises listed in STAR CCM+ documentation [3] for external aerodynamics; the geometry of the domain is presented below:

The domain was made using Boolean operations. The rectangular part next to the car is an equipment table which was present during measurements and was added to the domain for increased accuracy, as it changed the flow pattern around the car body. The inlet is a regular velocity inlet with velocity direction opposite to X-axis. The fluid leaves the domain through pressure outlet, for which all settings were left at STAR CCM+ defaults [3]. There is one natural symmetry plane pass-

ing through the middle of the car. The top and the right walls are also treated as symmetry planes..

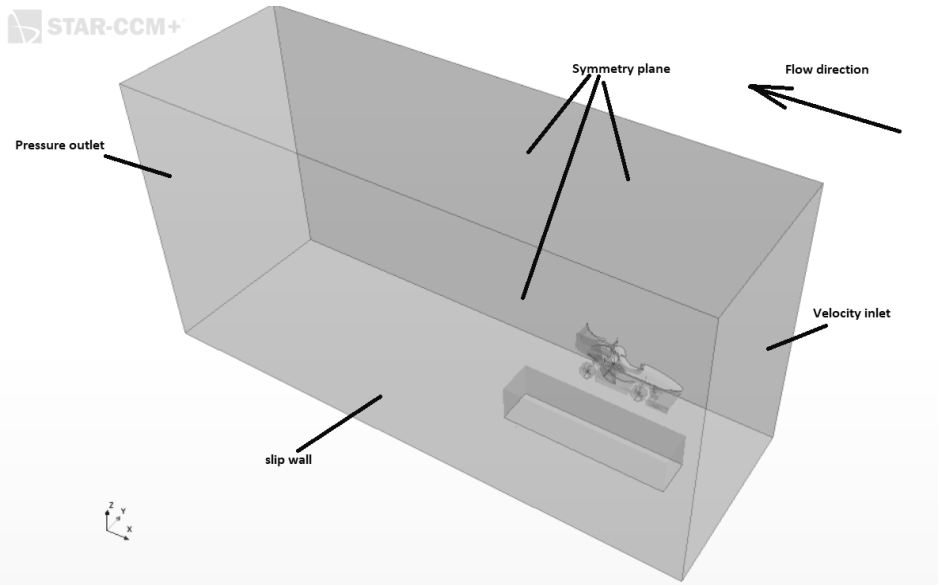


Fig. 2. Computational domain

This is because if they were treated as walls with no-slip condition, the mesh size would increase, and no difference in results was found. The domain is big enough so that the flow near these walls does not affect the results of the car, or at least not in a significant way. Another approach would be to treat them as pressure outlets, but again, no difference in results was found and it was causing several problems with convergence. In this case, symmetry plane is the fastest and most robust solution. The ground is modelled with a slip condition as the ground effects are of high interest in Formula Student cars, and their relative motion is kept this way. All car and table surfaces are treated as no-slip walls. The wheels are a rotating reference frame, and the radiator is a porous region. The radiator fans are modelled as if they were turned off. No heat generation is simulated. At the tip of the exhaust, there is a velocity inlet that copies exhaust gases exiting during engine operation. Also, the intake is simulated as a pressure outlet with negative pressure.

Other non-geometrical boundary conditions include:

- Constant density – Mach number is about 0.05
- Constant viscosity
- Constant temperature
- Turbulent, segregated flow
- Simulations were run at velocities between 6–7m/s to match experimental data

## 3. MESH

The mesh is created using automated mesh operation in STAR CCM+. It uses Trimmed Cell Mesher with Automatic Surface Repair and Prism Layer Mesher. The chosen approach was y+ < 1. We decided to use 13 to 16 prism layers on important surfaces that need boundary layer solution. This amount of prism cells enables STAR CCM+ to properly solve the boundary layer [3]. To save on mesh size, y+ value for suspension elements, engine, engine cage and wheels was 30 <y+ <150.

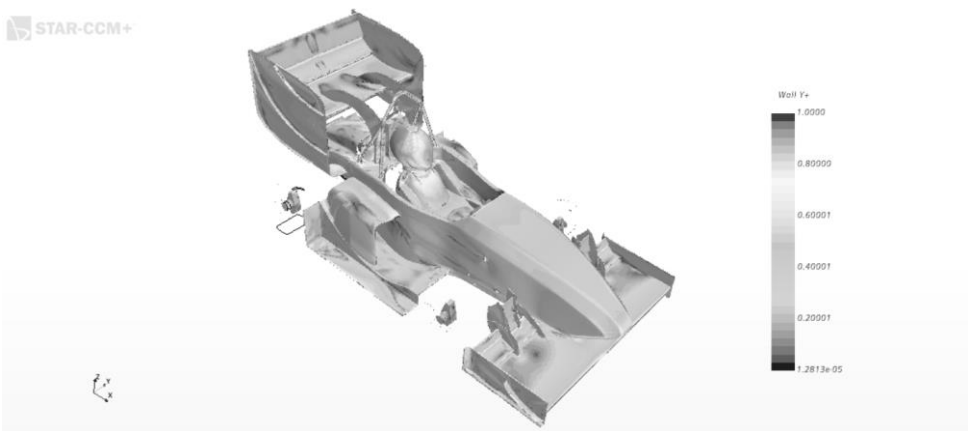


Fig. 3. low y+ elements

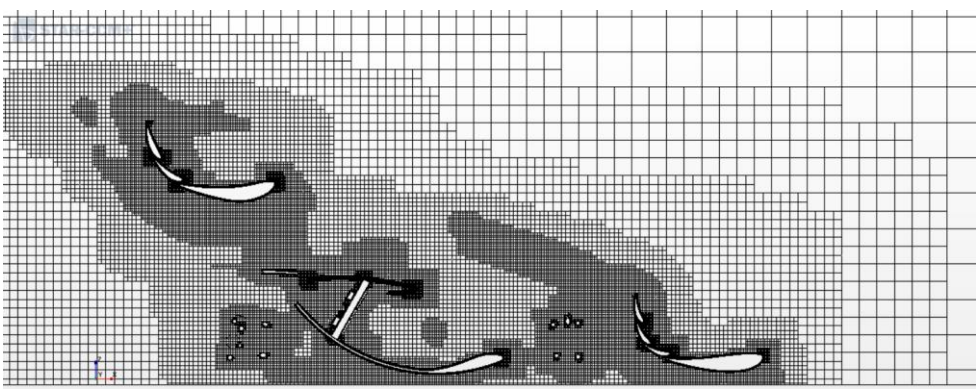

Fig. 4. Mesh form side

The total thickness of the prism layers was calculated using the flat-plate theory, and their thickness covers the whole boundary layer. With frequent changes in parts' geometry during the design of the Formula student car, we developed an adaptive mesh that refines regions that need more attention. Because of this, the

mesh presented in Figure 4 seems refined in odd areas. No volumetric controls are used, and initial simulation is run with only surface controls and automated volume mesh. After a given number of iterations, a new mesh is applied that refines regions with high gradients of turbulent kinetic energy and pressure. This allows for a comparison between simulations with different geometries, as the mesh is comparable. After refinement, the cell count is usually around 16 million. This mesh allows us to have residuals at around $1 * 10^{-6}$. It also allowed for residuals of front wing only simulations of around $1 * 10^{-9}$ and for solving adjoint cases.

## 4. PARTICLE IMAGE VELOCIMETRY

One of the many methods of visualising real flow and extracting data from it is Particle Image Velocimetry (PIV). It is a whole-field technique providing instantaneous velocity vector measurements in cross-section of flow. Basic measurements provide information about 2 velocity components of a fluid particle, while stereoscopic arrangement of cameras measures all 3 of them [1]. PIV uses lasers and lenses to produce a light sheet which acts as a cross-section plane. In the region of interest, seeding particles are introduced. These particles need to be chosen for a given application as their inertia, size, and scattering influence the results. While seeding particles are illuminated by laser light, a camera captures the image. The process of image capturing happens again after a short amount of time. These two pictures are then discretized. The amount of time between pictures being taken is so short that the path of particle can be approximated to a straight line with great precision. That path divided by time between the pictures gives instantaneous velocity vector:

$$\bar{V} = \frac{\Delta \bar{x}}{\Delta t} \tag{1}$$

Where:

V – velocity;
x – distance travelled;
t – time

The Adaptive PIV method used here is an automatic and adaptive method for calculating velocity vectors based on particle image pairs. The method can iteratively adjust the size, shape, and location of the individual interrogation areas (*IA*) in order to adapt to local seeding densities, as well as flow velocities and gradients. Each interrogation area produces one velocity vector. The method also includes options to apply window functions, frequency filtering, as well as a validation in the form of Universal Outlier Detection. Provided software calculates velocity

vectors with an initial interrogation area of the size *N* times the size of the final *IA*, and uses the intermediary results as information for the next *IA* of smaller size, until the final *IA* size is reached.

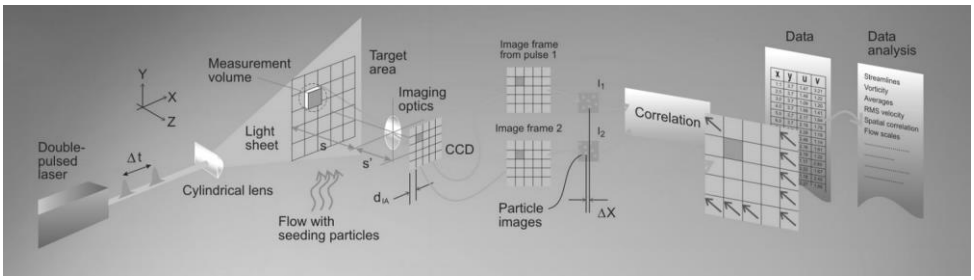


Fig. 5. PIV working principle [1]

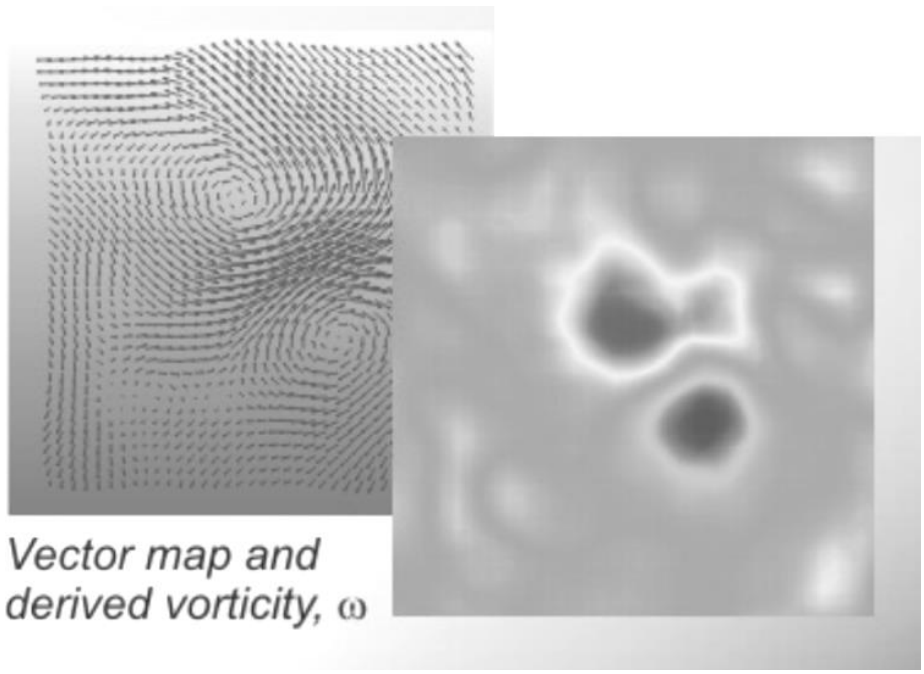


Fig. 6. Post processes PIV pictures [1]

Even though PIV captures instantaneous velocity components its results can be time averaged. Because of that highly dynamic phenomena can be validated even if RANS turbulence model was used. An example is given in Fig.7.

With advances in PIV technology the measurements do not need to be conducted in controlled environment of wind tunnels [2]. The flow can be captured in real conditions which greatly decreases the cost of this procedure. With correct ap-

proach the results will not differ in quality from those in wind tunnels while providing different point of view – moving body of interest, not air around it.

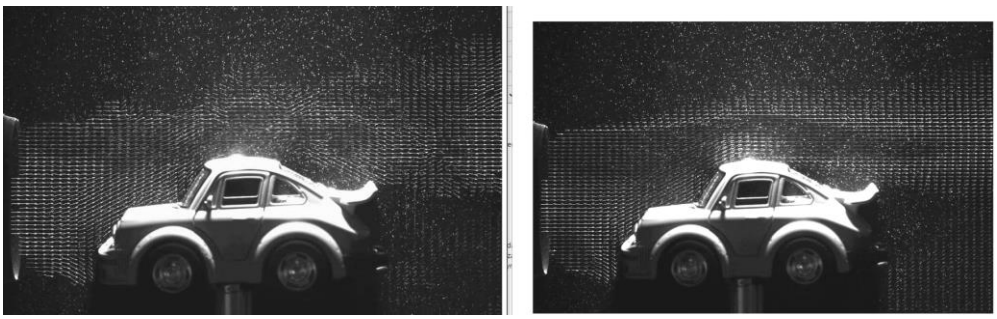

Fig. 7. Difference between time averaged flow on right side and instantaneous flow on left side [1]

## 5. MEASUREMENTS

All measurements were performed in industry production hall that was not occupied by any equipment at that time. This was a unique opportunity to try and run PIV tests in a real-world case. The floor was made of brushed concrete and because of that, it was very slippery, and the car was not able to reach a high speed. The highest recorded velocity was 7 m/s, and the majority of measurements was in range of 6–6.5 m/s, which corresponds to Reynolds number of 1 million. The hall was closed, and air conditioning was switched off, so no air movement was present. All tests were done with lights switched off, but daylight was entering the hall through roof windows. Laser and computers were placed on a table. The car was driving right next to it, but after including the table in CFD, the flow pattern could still be compared.


Fig. 8. Table with test equipment

In the Figure 8, a seeding particle generator is present, connected to air compressor. The placement of its outlet was critical to the quality of pictures. The oil mist produced by it was quickly dispersed in the volume of hall, and it was challenging to produce enough seeding particles in the area of interest. The lack of pneumatic installation in the hall greatly reduced the efficiency of said system, and air compressor flow rate was just enough. Between each run, the mist needed to be reintroduced to the testing area. All measurements were done using Dantec Dynamics laser form DualPower series designed for PIV, visualization, and particle sizing. The laser was powered by a manufacturer-provided 230 V power supply. It had a wavelength of 532 nm with pulse energy of 2x200 mJ for 5–9 ns. The laser and its power supply weight around 50 kg and were difficult to move. To have laser light illuminate the area of interest, a swinging arm with mirrors inside was used. To minimize light reflection and scattering, all reflective surfaces on the car were masked with black matte tape. This helped enhance image quality. Silver tape was used to mark each area of the car in order to recognize car position on images.


Fig. 9. RTX at the moment of laser activation

The final measurement stand consisted of a beam, under which the car was passing, and a swinging arm, also attached to the beam in a way that allowed to control its position and the angle of the lens. A camera was placed next to it to see exactly where the car was during given measurement. A measuring tape was placed on the ground for easier definition of laser light plane position in regard to the car. Before every measurement, a line was drawn on the ground for the driver to follow. The position of the lightplane was determined in static conditions. Two cameras were used for every passing of the car to capture more pictures; two camera set up would also allow to see all three velocity components, however, due to time limitations, no stereo pictures were taken. The laser was set at 30% of its power so that it was safe to work around it. When the laser was set to its operating power, drivers were equipped with safety glasses, and so was everyone working around the laser.

## 6. RESULTS

To compare the pictures easily, all CFD predictions are in GREEN and PIV results are in RED.

Starting from the front of the car, a slight separation region is visible behind the front wing flaps. It is marked in the red box in the picture below. As separation and its effect are difficult to predict for CFD, it is a region of great interest.

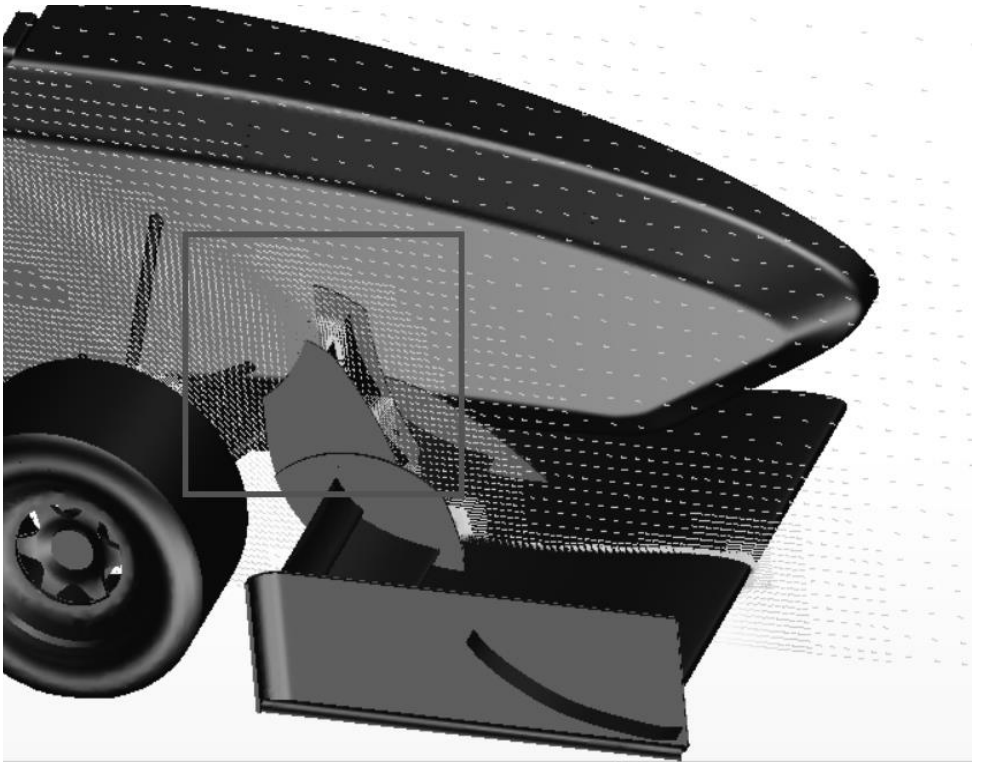

Fig. 10. Region of PIV pictures for front wing flaps

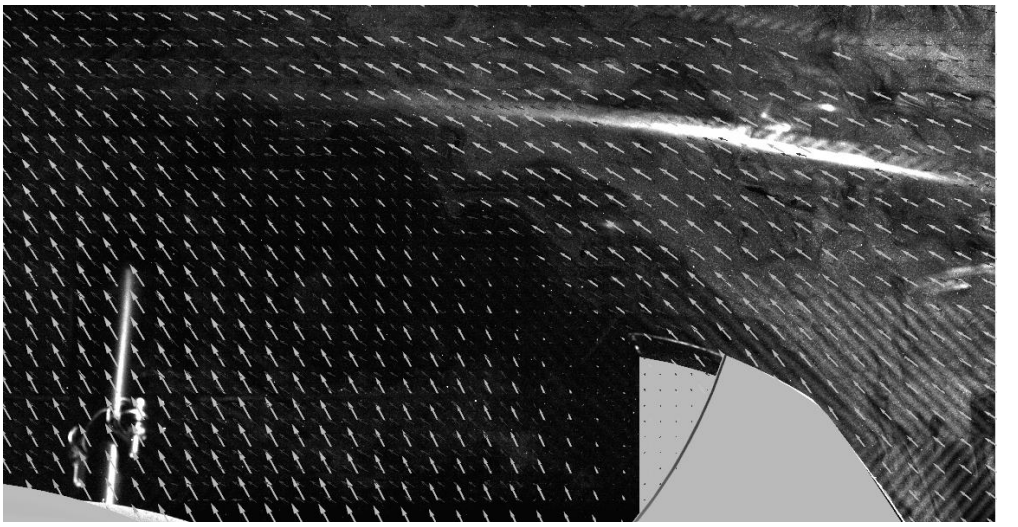

Fig. 11. Front wing Menter SST k-ω

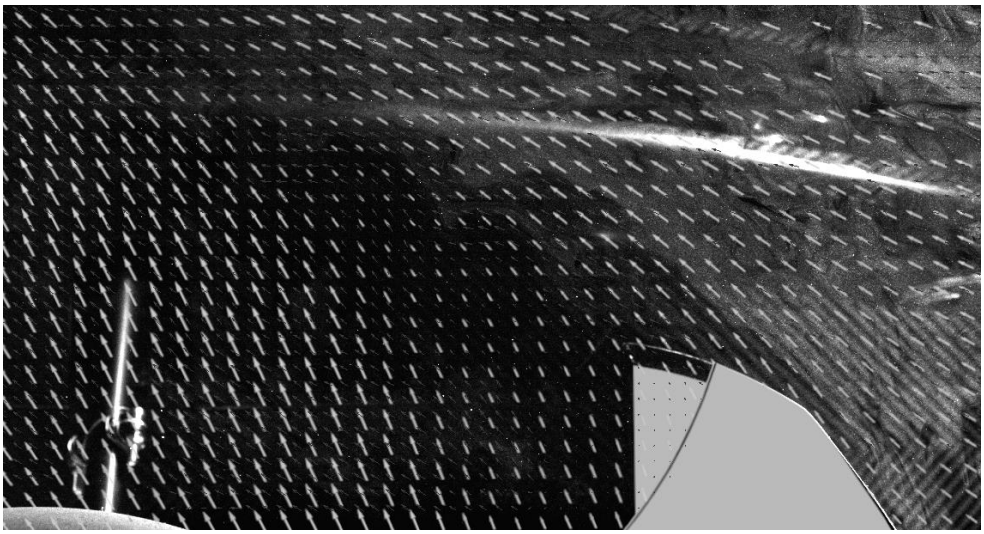

Fig. 12. Front wing Two-layer k-ε

The results are presented in Figure 11 and 12. The k-ω SST was used for Figure 11. It can be noticed that CFD predicts a separation and vortex behind the flaps. It correctly calculated the vortex to be rotating clockwise. However, the simulation fails at the prediction of the size of the vortex. The PIV picture shows that it is smaller than predicted by CFD and that the flow regains its velocity quicker than in the simulation. Because of that, the region behind that vortex differs in CFD. As can be seen on the left side of the picture, the position of the vectors predicted by CFD is more vertical compared to those captured by PIV. The overall convergence to reality of k-ω SST is still impressive, as the differences might just come down to time-averaging of CFD. The k-ε model presented in figure 12 completely skips the separation and predicts the flow to behave as if it was attached. There is a slight velocity decrease in the viscus wake, but it is far away from the wing surface, and in PIV picture, the air molecules have already reached free stream velocity. Just like in k-ω SST, the vectors on the left side of the picture are more vertical than those from PIV.

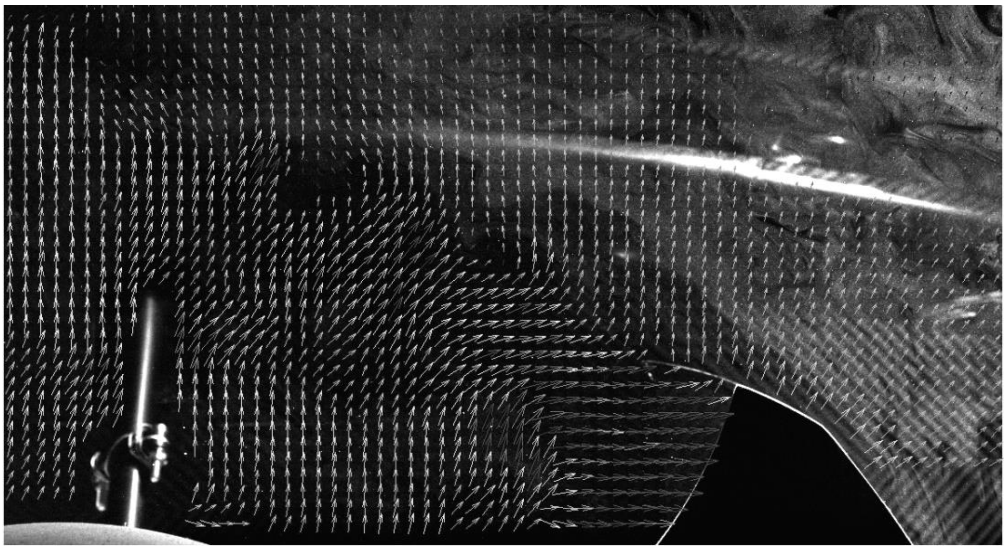

Fig. 13. Front wing PIV picture with real velocity field

In the picture above, the real velocity field can be observed. The separation here is the exact opposite of what can be seen in CFD. The air is moving towards the separation region in attempt to equalize the pressure distribution. In front of the wing, velocity has a component in the same direction as the car, which is a result of the "build-up" of air particles in front of the car as the pressure there is higher.

Another high interest region is the volume around the front and rear tires. They introduce unsteady wake of highly turbulent air, and a separation is ought to occur on their surface. Solvers usually predict a general shape of this turbulent wake, but not its details. In the picture below, the global flow field is well converged with PIV picture, and the volume of influence of the tire is similar to the real case. The wake itself is, however, difficult to compare because of time averaging carried our by CFD. The vortices present in the wake have a similar size to those in PIV, and air particles start to regain their velocity in the same place on the left. The CFD predicts this velocity recovery to be much slower than in the real case. The separation from tire surface is surprisingly accurate. The influence of reflective push rod surface is visible again as a region without PIV vectors just above the tire. What is interesting about the pictures below is that both k-ω SST and k-ε predict the flow to act almost the same. There is a slight difference on the left side where k-ε does not predict any velocity increase but besides that, the velocity fields are the same.

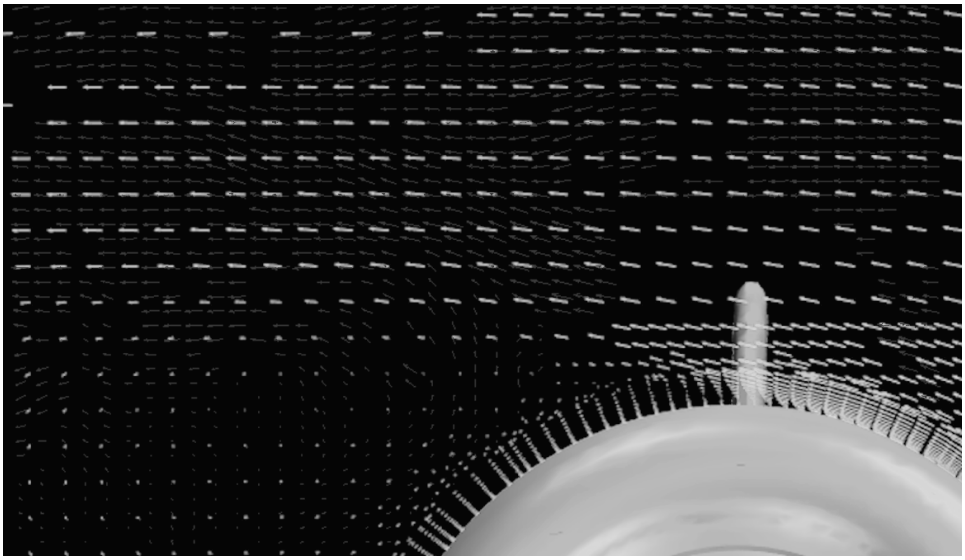

Fig. 14. Front tire with k-ω SST

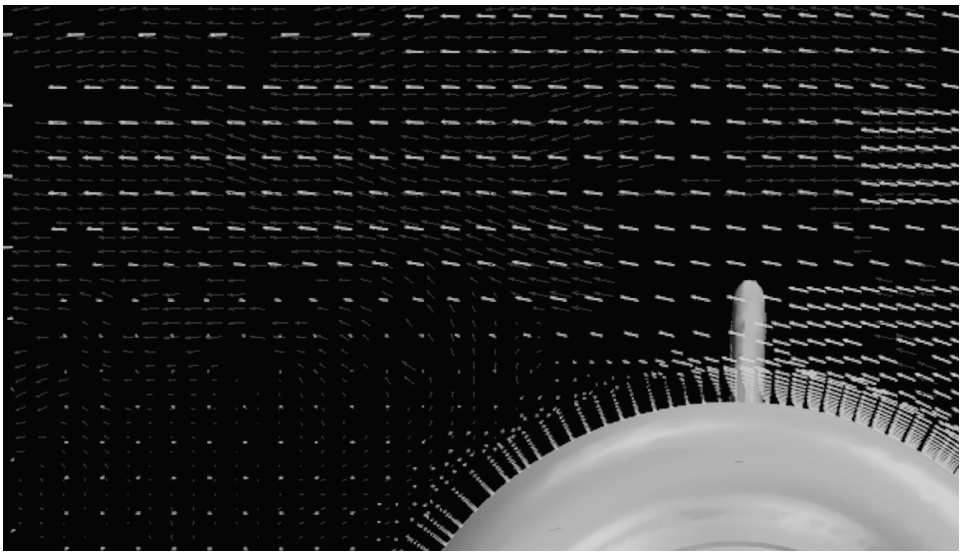

Fig. 15. Front tire with k-ε

The real flow field shown in Figure 16 shows the separation and the region with velocity in the same direction as the car. As the car has to move this mass of air, it creates resistance, and this is one of the reasons for the wake behind the tire to be considered adverse. Here, the tire wake seems to be very organized and almost laminar. The particles far above the tire are not influenced by the tire wake and seem to be undisturbed, even through they are affected by front wing upwash. Only

after subtracting the velocity of the car, a familiar vector field emerges with unsteady wake and some wake influence.

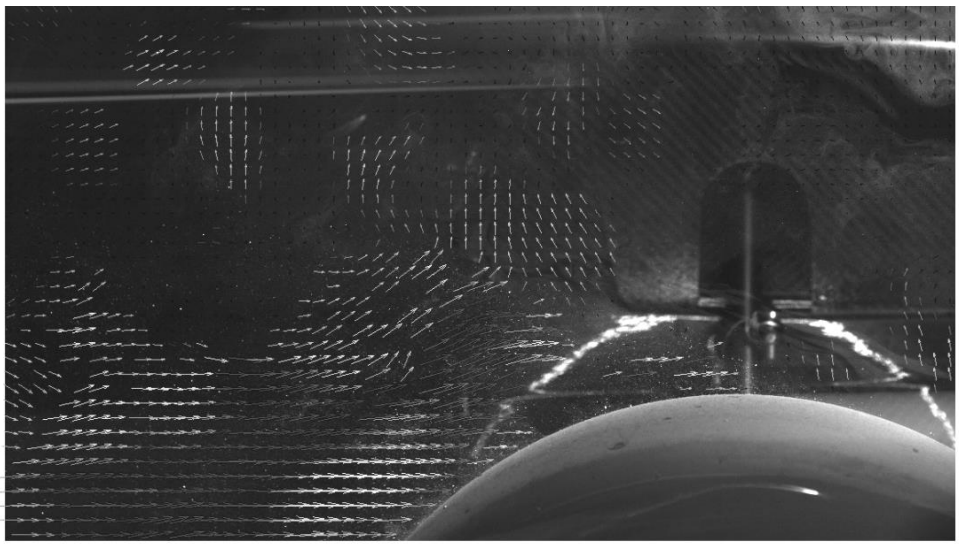

Fig. 16. Front tire real flow field

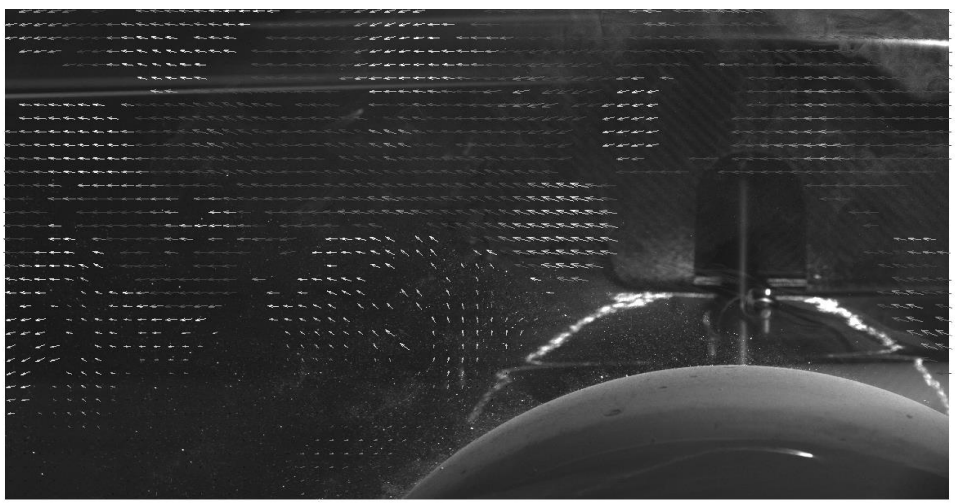

Fig. 17. Front tire with car velocity vector subtracted

Going further towards the back of the car, the flow field gets more and more complicated, and CFD starts to fail to properly predict fluid behaviour. The rear tire is a good example of a complex flow which is influenced by all the elements on the car. To properly simulate flow field around the rear tire, all elements in front of it must be calculated correctly, and the pressure field of the rear wing needs to be

convergent with the real world. For the real flow, there is a separation occurring on the tire surface, and the fluid velocity is very diverse as there is low energy fluid from cooling duct, front wing, and underbody wake. All of this is affected by low pressure behind the rear wing and its wing tip vortexes.

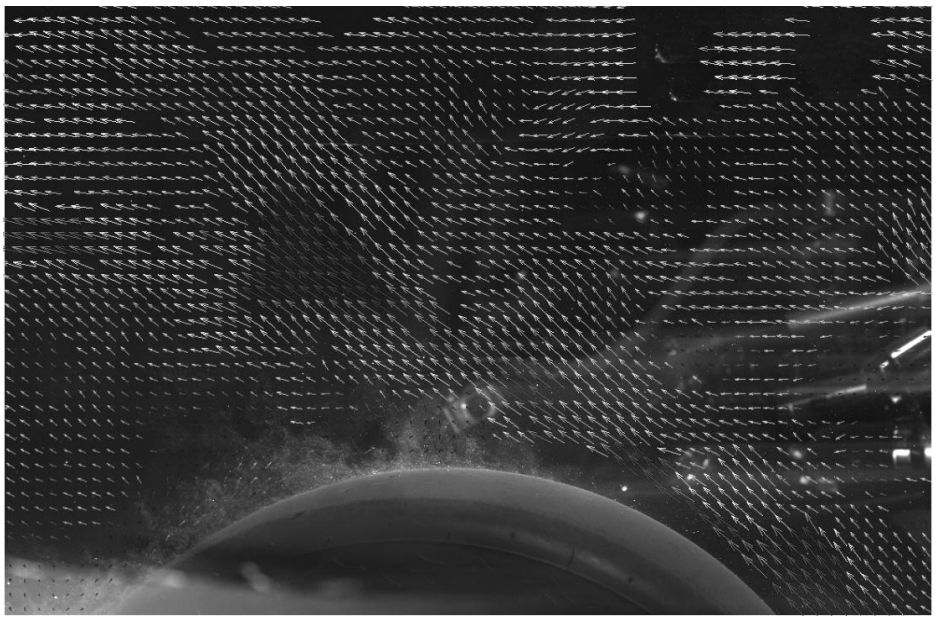

Fig. 18. Rear tire PIV picture with car velocity subtracted

CFD predicts the low velocity region on the right bottom corner, but fails to predict its size; as it is much bigger than in PIV pictures and overall, the velocities are underestimated. Furthermore, no separation seems to be occurring on tire surface. The boundary layer in CFD seems to be changing its shape to look more like adverse pressure velocity profile, but separation is not predicted. The eddy present on the left bottom side in Figure 18 is not to be found in neither k-ε nor k-ω SST simulations. It is clearly a problem with CFD calculations, as not predicting separation in such pressure gradient is not time-averaging fault. Perhaps the local reference frame was rotating in the opposite direction.

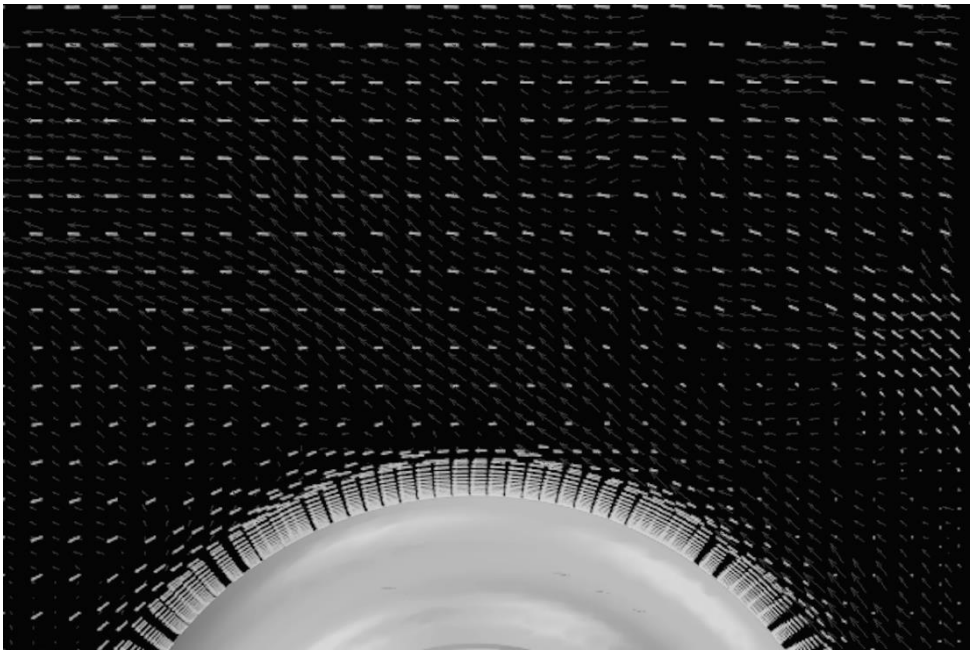

Fig. 19. Rear tire with k-ω SST, k-ε predicted same flow filed

## 7. CONCLUSIONS

All modern CFD require validation in a real-world scenario. While using CFD for CAE projects, the inaccuracy of turbulence models needs to be taken into consideration. With advancements in validation technology, the tests can become less expensive and time-consuming. PIV enables high-quality real-world testing with results comparable to regular wind tunnel at a fraction of the price. When talking about moving vehicles, real-case PIV also provides insight into the flow as it occurs in natural conditions. The pictures presented here show how much different the real-case flow is from the usual reference frame. The ability to see the real velocity field is only available while using PIV. The quality of pictures taken with PIV in production hall can be easily comparable with those taken in controlled wind tunnel environment. Even though post-processing of said pictures is more time-consuming, the data obtained allows for better understanding of actual flow fields, as well as CFD validation and fine tuning. The two most popular turbulence models show great resemblance in most cases, but in high performance wings, the k-ω SST predicted the flow much better than k-ε. The separation predicted by k-ω SST was accurate in most cases. The k-ε struggled to predict separation and even though most of the flow field was predicted correctly, the details are most important – and this is where k-ω SST came out better in this particular case.

## LITERATURE

[1] https://www.dantecdynamics.com/solutions-applications/solutions/fluid-mechanics/particle-image-velocimetry-piv/measurement-principles-of-piv/ 2019. (accessed: 25.05.2021)
[2] RAFFEL M., WILLERT C., WERELEY S., KOMPENNHANS J., *Particle Image Velocimetry A Practical Guide*, second edition, Springer, 2007
[3] SIEMENS, STAR CCM+ Users Guide, 2019

## WALIDACJA PRZEWIDYWANIA CFD DLA PRZEPŁYWU W PEŁNEJ SKALI FORMUŁY POJAZDU STUDENCKIEGO PRZY UŻYCIU PIV W RZECZYWISTYCH WARUNKACH

**Słowa kluczowe:** *aerodynamika, CFD, walidacja, PIV, Velocymetria obrazu cząstek, student wzoru*

Prognozy obliczeniowej dynamiki płynów (CFD) stają się standardem branżowym. Pozwalają na dokładne przewidywanie złożonych problemów bez konieczności przeprowadzania rozległych testów w warunkach rzeczywistych, oszczędzając czas i pieniądze. Jednak wiele razy zostało udowodnione, że klasyczne podejście Reynoldsa uśrednione Navier-Stokes (RANS) ma swoje wady i nie zapewnia bardzo dokładnych prognoz. Mimo że CFD zbliża się tylko do rozwiązania fizycznego i może osiągnąć je tylko w bardzo specyficznych zastosowaniach, do celów inżynieryjnych zwykle zapewnia wystarczającą precyzję. Aby osiągnąć zbieżność z rzeczywistą fizyką, należy wziąć pod uwagę wiele czynników, takich jak siatka, warunki brzegowe i modele turbulencji. Aby mieć symulację CFD, która dokładnie odzwierciedla rzeczywistą fizykę, musi nastąpić pewnego rodzaju walidacja w prawdziwym świecie. Zwykle odbywa się to w tunelach aerodynamicznych, jeśli mówimy o aerodynamice, które są drogie w eksploatacji, ale zapewniają kontrolowane warunki, aby dopasować się do tych określonych w CFD. Jedną z wielu metod stosowanych do walidacji obliczeń jest Velocymetria obrazu cząstek (PIV). To badanie próbuje zweryfikować CFD samochodu Formula Student przy użyciu PIV, ale w rzeczywistych warunkach, bez tunelu aerodynamicznego. Umożliwiają to kompaktowe rozmiary sprzętu wymaganego do testów PIV i elastyczność warunków brzegowych CFD.